**Noname manuscript No.**
(will be inserted by the editor)

# Statistical property of small particle trajectories in fully developed turbulent state of HeII

**Wataru Kubo · Yoshiyuki Tsuji**

Received: date / Accepted: date

**Abstract** Lagrange trajectories of small particle in fully developed turbulent state are studied in rectangular duct. The plate heater is attached on the bottom to generate the thermal counter flow. The bass temperature is changed from 1.7K to 2.1K, and it is controlled within 0.1mK. The small particles made of solid hydrogen are visualized by high-speed camera and their trajectories are recorded. Not only depending on bath temperature and heater power, but also depending on their particle sizes, their motions indicate complicated features. In this study, the Hurst exponent defined by $|\mathbf{x}(t+\tau)-\mathbf{x}(t)| \propto \tau^H$, where $\mathbf{x}(t)$ denotes the particle position at time $t$. It was found that there is a typical time scale $\tau_0$. In small time separation; $\tau \leq \tau_0$, the exponent $H$ is small however for large time separation; $\tau_0 \ll \tau$, $H$ is nearly 1.

**Keywords** Lagrange velocity · particle size · PTV measurement

## 1 Introduction

Turbulence of Helium is an interesting research area and it is important both in fundamental science and applications [1-2]. Below the temperature 2.17 K, liquid Helium is called HeII in which no-viscosity super fluid exist together with normal fluid depending on the bath temperature. Superfluid exhibits the behavior similar to that found in a classical fluid, but it may take forms that are unknown in classical fluid once the quantized vortices are generated and mutual friction appears.

In the recent decade, new techniques have been applied to visualize the flow of superfluid helium and measure the local velocity fluctuation. Among them the convenient ones are particle image velocimetry (PIV) and particle tracing

Y. Tsuji
Tel.: +81-52-7894693
Fax: +81-52-7894692
E-mail: c42406a@nucc.cc.nagoya-u.ac.jp

velocimetry (PTV) techniques [3], which are potential tool to measure local velocity and promises to provide a deeper understanding of complex superfluid motions.

In our previous research, particle motions were analyzed by PTV technique [4]. Small particles are made of solid Hydrogen, whose diameter is in the order of $\mu$m. Particles are carried by normal fluid due to the fluid viscosity and they are also trapped by quantum vortexes. The interaction of normal fluid with quantum vortex leads to make the complicated particle motions. We have reported that the particle motions are affected by the particle sizes. That is, smaller particles tend to be trapped by quantum vortexes, and larger particles are carried by background flow independent on super fluid. In classical turbulence, it is well known that the particle motions are affected by their particle sizes. This problem has been studied so far by experiments and numerical simulations. They are characterized by $St$ number defined by the ratio of the particle inertial response time to the time scale of the smallest eddies. When the $St$ number is sufficiently small, the particle motions are not affected by their sizes [5]. Small scale vortexes are not clearly identified in classical turbulence, and they do not trap the particles. Therefore, the small-scale particle motions might be different in quantum turbulence.

In the present study, small tracer parties in HeII are visualized and their Lagrangian motions are analyzed. The particles are made of solid hydrogen whose diameter is on the order of microns, which is the same method developed by previous researches [6-7]. In a thermal counterflow, changing the heat flux and bath temperature, Lagrangian velocity and accelerations are computed by analyzing the visualized images through the PTV technique. We discuss the dependence of Lagrange velocity and acceleration on the particle sizes. And Lagrange trajectories are analyzed from the view point of Fractional Brownian motions [8]. Particle motions do not indicate the Brownian motions but slightly different peculiar behaviors. We evaluate the typical time scale caused by the small vortex angles, and the vortex line density is estimated.

## 2 Experimental condition

Inside the dewar, the schematic view is shown in Fig. 1, the rectangular channel (cross section is $A = 50 \times 55$ [mm$^2$] and the height is $H = 115$ [mm]) made of glass is placed. The bath temperature $T_B$ is varied from 1.7 to 2.1 [K]. The plate heater is located at the bottom, and the heat flux $q$ is set at 200, 400, 600, and 800 [W/m$^2$]. Then the thermal counterflow is generated inside the duct. A high-speed camera ($1024 \times 1024$ pixels, 12 bit) is used for visualizing the area $8.7 \times 8.7$ [mm$^2$] at 250 [fps]. A continuous laser (wave length 532 [nm], Diode Pumped Solid State laser) is used to generate laser sheet with a thickness of about 1 [mm]. The typical four cases are analyzed in this study as summarized in Table.1.

In this study, we adopt the condensation and dispersion of solid hydrogen particulates from the gas phase. A helium and hydrogen mixing chamber is

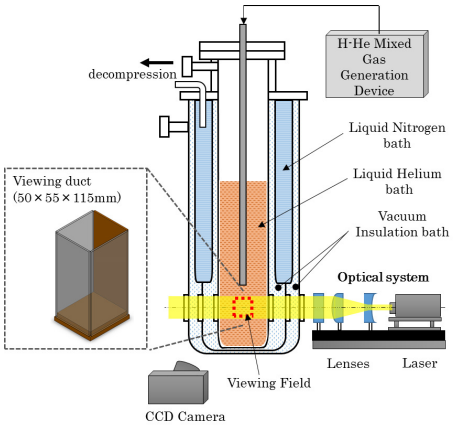


**Fig. 1** Schematic view of experimental apparatus (Color figure online).

**Table 1** Experimental conditions

| case | bath temperature T [K] | Heater power[W/m$^2$] |
|---|---|---|
| case A | 2.10 | 400 |
| case B | 2.02 | 420 |
| case C | 1.76 | 420 |
| case D | 2.08 | 780 |

designed to change the mixing ratio and the spouting pressure, and hydrogen particles are generated in the liquid helium. The condition that the mixing ratio is He:$H_2$ = 40:1 and injection pressure is 20k [Pa]. The injection is done just above the $\lambda$ pint and then decreases the bath temperature. The temperature is controlled with 0.1mK by controlling the bath pressure. The particle trajectories are analyzed by image processing techniques. The algorithm was improved from the previous researches [5] and can track the particle motions depending on the particle sizes. But the present algorithm does not analyze the vortex reconnection process. Thus, the trajectories close with each other are not taken into account in this study.

## 3 Results and Discussions

Before analyzing the particle trajectory, the particle sizes are calibrated by the nylon particles (Kanomax Nylon Particle Model 0456). Their density is $\rho$ = 1.02 g/cc and the diameter is 4.1 $\mu$m in average. The particles are spread in the pure water and then mixed together. The slow particle motions are generated. Imaging system is the same with that used in He experiment as mentioned in section 2. Figure 2a shows the particle trajectories in which the different colors correspond to different particle trajectories and back solid circle locates at the starting point of each trajectory. The distribution function of particle sizes

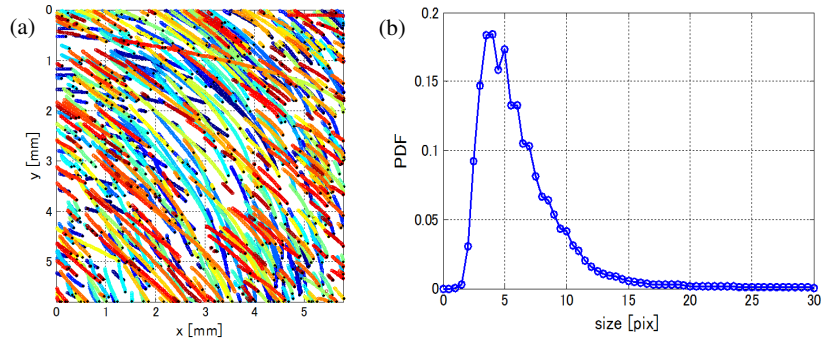


**Fig. 2** (a) particle trajectory, (b) particle size distribution (Color figure online).

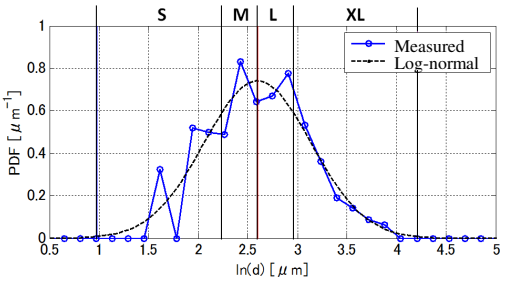


**Fig. 3** Log-normal distribution of particle size in HeII . (Color figure online).

is plotted in Fig.2b. The particle sizes distribute from 2.0$\mu$m to 15$\mu$m. The peak value is about 4.6$\mu$m. Velocity profile, which is not shown here, is well approximated by Gaussian distribution. From these results, we may conclude that the present imaging system capture the particle sizes accurately.

The distribution function of solid $H_2$ particles is plotted in Fig. 3. Instead of particle sizes $d$ for itself, the logarithm of $\ln d$ is analyzed. The distribution is approximated by Gaussian profile, therefore, the particle sizes are nearly log-normal distribution. In the following analysis, we divide particles into four groups S ($a - 3\sigma \leq \ln d < a - 0.67\sigma$), M ($a - 0.67\sigma \leq \ln d < a$), L ($a \leq \ln d < a + 0.67\sigma$), and XL ($a + 0.67\sigma \leq \ln d < a + 3\sigma$) for convenience, where $a$ is average and $\sigma$ is standard deviation. In this partition, each size has 25% of probability.

Figure 4 shows the velocity distribution in vertical (y) direction. The different colors indicate the different particle sizes. There are double peaks which corresponds to the particle motion trapped by normal and super fluid components, respectively. The normal fluid is positive and super fluid represents the negative value. The dashed lines are theoretical values derived by two fluid model [1,2], which are expressed as $v_{s,th}$ and $v_{n,th}$ for suer and normal fluid, respectively, The measured normal velocity distribution is smaller than $v_{n,th}$ and the super one is larger than $v_{s,th}$. The double peaks are observed

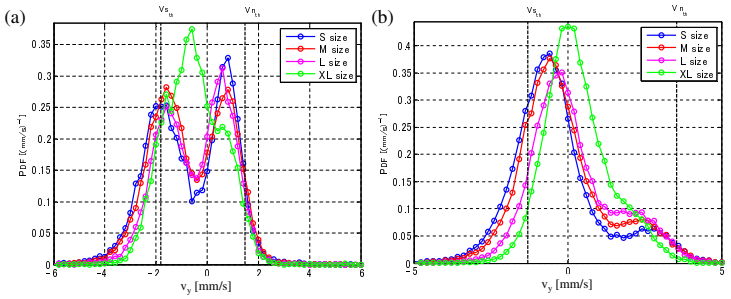


**Fig. 4** Velocity profile in y-direction. (a) case B, (b) case C. (Color figure online).

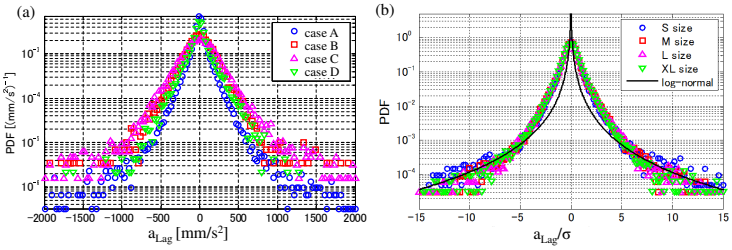


**Fig. 5** Lagrange acceleration in y-direction profile. (a) S size (b) case A. Solid line is log-normal distribution; $P(a) = \frac{\exp(1.5S^2)}{4\sqrt{3}}\left[1 - erf\left(\frac{\ln|a/\sqrt{3}|+2S^2}{\sqrt{2}S}\right)\right]$ with $S = 1.5$. (Color figure online).

for size of S, M, and L. It is noted that the velocity profiles are depending on the particle sizes. In the case of C, both normal and super fluid components vary clearly depending on the particle sizes. However, the particles of XL size has a single peak. That is, they move up and down not affected by the background normal and super fluid flow. The velocity profiles in horizontal (x) direction, which are not shown here, have single peak distributions and overlap sufficiently independent of particle sizes. Although their fluctuations are small $|v_x - a| \leq 1$[mm/sec], where $a$ is an average of $v_x$, they are not negligible compared with those of vertical components. Thus, the background flow is not laminar but turbulent. And the theoretical mean velocity value does not agree with the peak of measured velocity profiles.

The Lagrange particle acceleration $\mathbf{a} = (a_x, a_y)$ is calculated from the continuous three particle positions $p_1(x_1, y_1)$, $p_2(x_2, y_2)$, and $p_3(x_3, y_3)$ sampled at $\Delta t$ interval by way of second-order accurate central-difference scheme. And the component along the path of line, $a_{Lag}$, is analyzed. Figure 5 shows the probability density function (PDF) of acceleration. The axes are normalized by the standard deviation and the solid line is log-normal distribution. The PDF has a long tail part. This feature has been observed in previous researches. Long tail corresponds to the intermittent events with large acceleration. Particles are trapped by vortexes and move downward to the heater side. They

are sometimes detrapped, change its direction and carried by normal fluid. In this case, acceleration become large. Another high-acceleration event is a reconnection of vortexes. When the vortexes approach close to each other with some speed, the reconnection happens. Small particles trapped by vortex are suddenly changes its position. In the present PTV analysis, the reconnection events are not taken into account. The tail of PDF is close to the log-normal distribution, however the core region is not. The PDFs overlap sufficiently if normalized its standard deviation, then the particle sizes do not affect the PDF profile. This is contrary to the velocity PDF. In classical turbulence, the acceleration statistics have been studied so far in experiments and numerical simulation [5]. The PDF shape depends on the $St$ number defined by the ratio of the particle inertial response time to the time scale of the smallest eddies. For smaller $St$ number, the tail extends broader. Figure 5a shows the temperature dependence of acceleration PDF. The tail parts become broad for lower temperature. That is, the intermittent events, occurring in small probability, affect strongly the acceleration as temperature decreases.

Studying the Lagrange trajectory in detail, the increment of trajectory defined as $\Delta x(\tau) = |\mathbf{x}(t+\tau) - \mathbf{x}(t)|$ is analyzed, where $\mathbf{x}(t)$ is a particle position at time $t$ and $\tau$ is a time lag. In a statistical sense, we can expect the following power-law relation.

$$\left\langle |\mathbf{x}(t+\tau) - \mathbf{x}(t)|^2 \right\rangle = C\tau^{2H} . \tag{1}$$

Here, the angle bracket is the ensemble average, $C$ is constant parameter and the power-law exponent $H$ is called Hurst exponent [8]. It varies between $-1 \leq H \leq 1$. In the case of $H = 1/2$, particle motion is Brownian motion and the increment $\Delta x$ is independent random variable. For $H = 1$, the particle motion is a linear motion and the increment is constant value. In general, the motion is called fractional Brownian motion if Eq. (1) is satisfied among the appropriate range of $\tau$. The increment has a positive correlation for $1/2 < H < 1$ and negative correlation for $0 < H < 1/2$.

The variance of $\Delta x$ is plotted in Fig. 6 for different particle sizes. The slope corresponds to the exponent $2H$. It is found that there is a typical time scale $\tau_0$. In small time separation; $\tau \leq \tau_0$, the exponent $H$ is small however for large time separation; $\tau_0 \ll \tau$, $H$ is nearly 1. The particle motions in small time separation might be affected by the quantum vortex, and the motions in large time scale are carried by background flow. The exponents are 0.54, 0.68, and 0.61 for S, M and L particle sizes, respectively. That is, S size particle has more complicated trajectories rather than those of M and L sizes, but XL particle does not have an interaction with quantized vortexes. For large time separation, the exponents are 0.96, 0.97, 0.87, and 0.98 for S, M, L, and XL sizes, respectively. The smaller sizes have a larger exponent. Therefore, the smaller particle indicates near the liner motions. The typical time scale $\tau_0$ slightly increases as particle sizes become large.

The Hurst exponents and transition time scales are analyzed for Case A-D. It is found that Hurst exponents have smaller values for lower bath temperatures. Also, the transition time is small for lower temperatures. Therefore,

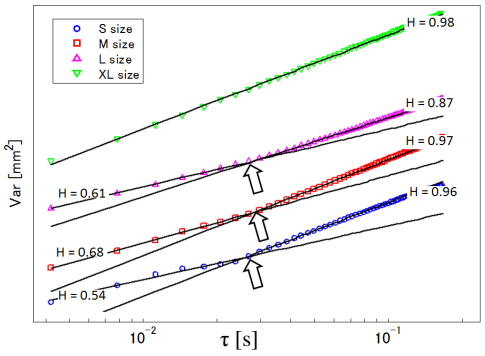


**Fig. 6** Variance of particle motions against the time tag. The arrow indicates the tansition time scale $\tau_0$ (case A). (Color figure online).

the interaction between particles and quantized vortexes are strong in lower temperatures. Transition time scale $\tau_0$ is changed into length scale $\ell$ by using the relative velocity $v_{ns}$ as $\ell = v_{ns}\tau_0$, where $v_{ns} = |v_n - v_s|$. Here, normal velocity $v_n$ and super fluid velocity $v_s$ are adopted as $v_{n,th}$ and $v_{s,th}$, respectively. Then the vortex line density $L$ is calculated as $L = 1/\ell^2$. $L$ is $4.4 \times 10^3$, $9.4 \times 10^3$, and $1.7 \times 10^4$ [cm$^{-2}$] for case A, B, and C, respectively. The vortex line density in the present study is the same order with that of previously reported researches [9].

**Acknowledgements** Financial support from the Japan Society for the Promotion of Science 15H03917 and Challenging Exploratory Research 16K14158 are gratefully acknowledged. The experimental support by Mr. Akira Hirano, Mr. Daiki Kato and Kouhei Oodaka were indispensable in our measurements.

## References

1. W. F. Vinen and J. J. Niemela, Quantum turbulence, Journal of Low Temperature Physics 128,167 (2002).
2. C. F. Barenghi, L. Skrbek, and K. R. Sreenivasan, Introduction to quantum turbulence, Proc. Natl. Acad. Sci. USA 111, 4647 (2014).
3. R. J. Adrian and J. Westerweel, Particle Image Velocimetry, Cambridge University Press, (2011).
4. W. Kubo and Y. Tsuji, Lagrangian Trajectory of Small Particles in Superfluid He II, Journal of Low Temperature Physics, 187, 611(2017).
5. F. Toschi and E. Bodenschatz, Lagrangian Properties of Particles in Turbulence, Ann. Rev. Fluid Mech., 41, 375(2009).
6. M. La Mantia and L. Skrbek, Quantum turbulence visualized by particle dynamics, Phys. Rev. B 90, 014519 (2014).
7. B. Mastracci and W. Guo, Exploration of thermal counterflow in He II using particle tracking velocimetry, PHYSICAL REVIEW FLUIDS 3, 063304 (2018).
8. B. B. Mandelbroat and J. W. Van Ness, Fractional Brownian Motions, Fractional Noises and Applications, SIAM, 10, 422(1968).
9. S. Yui, M. Tsubota, and H. Kobayashi, Three-Dimensional Coupled Dynamics of the Two-Fluid Model in Superfluid 4He: Deformed Velocity Profile of Normal Fluid in Thermal Counterflow Physical. Rev. Lett., 120, 155301 (2018).